

Buffer layer-enhanced magnetic field effect in manganite-based heterojunctions

W. M. Lü, J. R. Sun,^{a)} Y. Z. Chen, D. S. Shang, and B. G. Shen

Beijing National Laboratory for Condensed Matter Physics and Institute of Physics,
Chinese Academy of Sciences, Beijing 100190, People's Republic of China

(Received 26 September 2009; accepted 20 November 2009; published online 11 December 2009)

Influence of magnetic field on the rectifying property of the $\text{La}_{0.67}\text{Ca}_{0.33}\text{MnO}_3/\text{LaMnO}_3/\text{SrTiO}_3:0.05 \text{ wt \%Nb}$ heterojunctions has been studied. In addition to an enhanced magnetic response of the current-voltage characteristics, a field-induced increase in junction resistance, which is an effect different from that in the junctions without the LaMnO_3 layer, is observed. The positive magnetoresistance is further found to show a systematic variation with the thickness of the LaMnO_3 layer (t), growing rapidly with the increase of layer thickness and getting a maximum of $\sim 91\%$ at $t=4 \text{ nm}$ ($T=50 \text{ K}$ and $\Delta H=5 \text{ T}$). Analysis of the current-voltage and capacitance-voltage characteristics indicates a field-induced growth of interfacial barrier, which is responsible for the abnormal effect observed here. © 2009 American Institute of Physics. [doi:10.1063/1.3273375]

Because of the strong magnetic-conductive correlation in manganites,¹ magnetic field is expected to have an important impact on manganite-based junctions. Due to the presence of an interfacial layer that is insensitive to external field,² however, the influence of magnetic field on the current-voltage characteristics, when they are dominated by thermionic emission, is rather weak,^{3,4} though tunneling or leakage current enhances considerably.² Moreover, in addition to the magnetic-conductive coupling, the order-disorder transition of the spin, orbital, and charge degrees of freedom of the manganites has also been severely depressed in manganite junctions. To incorporate the distinctive features of the manganite into corresponding devices, an approach that can depress the unexpected interface effect has to be explored. Recently, Yamada *et al.*⁵ found that the interfacial ferromagnetism of the $\text{La}_{0.6}\text{Sr}_{0.4}\text{MnO}_3$ film can be significantly enhanced by a neighboring LaMnO_3 layer. This suggests a possibility to modify interfacial properties of the junction by introducing a proper buffer layer. In this letter, we report a comprehensive study on the effect of magnetic field on the $\text{La}_{0.67}\text{Ca}_{0.33}\text{MnO}_3/\text{LaMnO}_3/\text{SrTiO}_3:0.05 \text{ wt \%Nb}$ (LCMO/LMO/STON) junctions. The magnetic field effect is greatly modified by buffer layer. In addition to an enhanced magnetic response of rectifying behavior, a field-induced growth in junction resistance, which is an effect completely different from that observed in the junctions without a buffer layer, is observed. This effect is further found to vary systematically with the LMO layer, and the strongest effect occurs at the layer thickness of $\sim 4 \text{ nm}$.

The LCMO/LMO/STON junction was fabricated by growing, via pulsed laser ablation, first a LMO layer with a thickness between 0 and 12 nm then a LCMO film of $\sim 150 \text{ nm}$ on (100) STON substrate. The substrate temperature was kept at $700 \text{ }^\circ\text{C}$ and the oxygen pressure at $\sim 10 \text{ Pa}$ (for the LMO film) or $\sim 80 \text{ Pa}$ (for the LCMO film) during the preparation. The film thickness was controlled by deposition time. For sample characterization, LMO and LCMO films with the thickness of the corresponding layers in

LCMO/LMO/STON were also prepared on SrTiO_3 substrates. The out-of-plane lattice constant of the LMO film is $\sim 0.399 \text{ nm}$, as evidence by x-ray diffraction.

The atomic force microscope analysis shows that the buffer layer is quite smooth with a terrace-structured surface. The root-mean-square roughness is, for example, for the LMO layer of 8 nm, $\sim 0.3 \text{ nm}$, and the peak-to-valley fluctuation is below $\sim 0.5 \text{ nm}$. It guarantees the high crystal quality of the top LCMO film. The LCMO film grown on SrTiO_3 shows a metal-to-insulator transition at $T_C \approx 245 \text{ K}$. Magnetic field depresses the resistivity of the film, and a field of 5 T produces a negative magnetoresistance (MR) of $\sim 90\%$ around T_C . In contrast, the LMO films are semiconductive down to $\sim 150 \text{ K}$, below which the resistance exceeds the scope of our devices. These behaviors are similar to those of bulk LCMO or LMO, respectively.¹

The current (J)–voltage (V) curves were measured, using a two-probe configuration. Two Cu pads of the size of $1 \times 1 \text{ mm}^2$ were deposited, also using laser ablation, respectively, on LCMO and STON as electrodes. The resistance is $\sim 100 \text{ } \Omega$ for the Cu-LCMO contact and $\sim 10 \text{ } \Omega$ for the Cu-STON contact. Electric bias directing from LCMO to STON is defined as positive. At a first glance, the LMO layer does not affect the junction, and excellent rectifying behavior persists in LCMO/LMO/STON. The rectifying ratio is 3.8×10^4 for, for example, $t=6 \text{ nm}$, obtained at the bias voltage of $|V|=0.5 \text{ V}$ and the temperature of 350 K. The semi-logarithmic J–V curves of LCMO/LMO(t)/STON for $t=1, 4, \text{ and } 6 \text{ nm}$ are presented in Figs. 1(a)–1(c). A linear relation between $\log J$ and V , $\log J \propto eV/nk_B T$, is observed when the LMO layer is below 6 nm, where e is the electron charge, k_B the Boltzmann constant, and n the ideality factor. This result reveals the good description of the Shockley equation for the electronic process in the junctions. Unlike the ones for $t < 6 \text{ nm}$, the junction with a buffer layer of 6 nm shows two distinctive processes, and the junction of $t \geq 10 \text{ nm}$ exhibits the leakage process-dominated J–V characteristics (not shown). The ideality factor of the junctions is shown in Fig. 1(d). It displays a growth from ~ 1.1 to ~ 2 as temperature decreases from 350 to 80 K. Its adjacency to unity and insensitivity to temperature above 200 K manifest the high

^{a)}Author to whom correspondence should be addressed. Electronic mail: jrsun@g203.iphy.ac.cn.

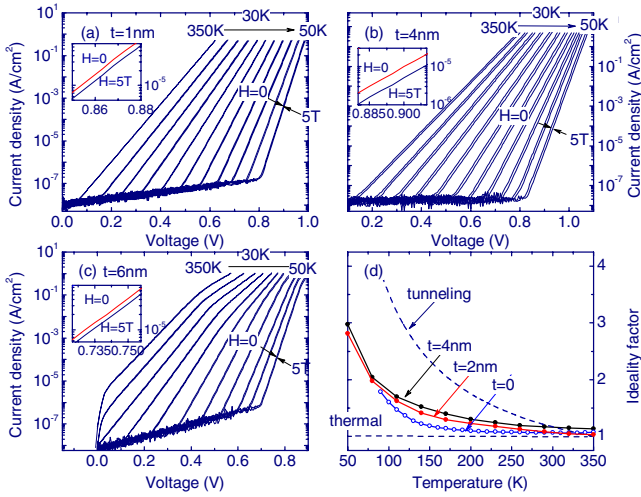


FIG. 1. (Color online) Semilogarithmic plot of the current-voltage characteristics measured with and without magnetic field for the LCMO/LMO(t)/STON junctions with $t=1$ nm (a), 4 nm (b), 6 nm (c), and the ideality factors of the typical junctions as functions of temperature (d). The bottom cut-off of the J–V curves is due to the limit of our ammeter. Inset plots are exemplified close views of the variation of the J–V curves in magnetic field.

quality of the junctions and the thermionic emission characters of the transport process.

As expected, the junction with an ultrathin buffer layer is insensitive to magnetic field, and changes in the J–V relations are very small even for a field change of 0–5 T [Fig. 1(a)]. The strongest effect appears in the junctions of $t=4$ nm, shown by an obvious downward shift of the logJ–V curve upon the application of magnetic field [Fig. 1(b)]. However, a LMO layer exceeding 6 nm depresses the magnetic field effect again [Fig. 1(c)]. In contrast, the J–V characteristics of LMO/STON are dominated by leakage current, without visible response to magnetic field.

Figure 2 illustrates the MR, defined as $J(0)/J(5T)-1$, as a function of positive bias for selected junctions $t=4$ and

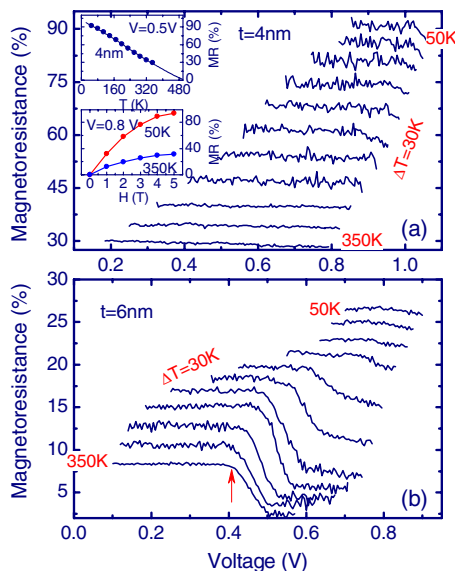


FIG. 2. (Color online) MR as a function of bias voltage for the LCMO/LMO(t)/STON junctions with $t=4$ nm (a) and 6 nm (b). The two inset plots present the temperature and magnetic field dependence of the MR, respectively. Arrow marks the critical voltage of the electronic transition.

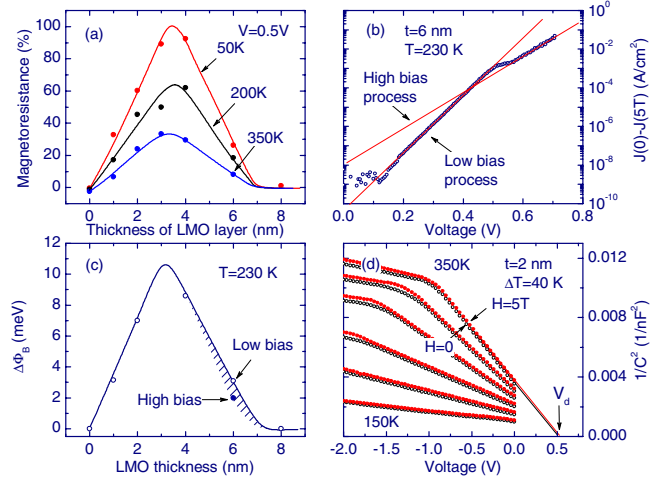


FIG. 3. (Color online) (a) MR as a function of the LMO layer thickness, obtained under the bias voltage of 0.5 V. The data for $t=6$ nm are obtained from the low bias process. (b) Field-induced current change as a function of bias voltage for the sample $t=6$ nm, obtained at the temperature of 230 K. (c) Field-induced variation of interfacial potential as a function of the LMO layer thickness. Shaded area marks the difference of the high and low bias processes. (d) Reciprocal square capacitance as a function of bias voltage for the LCMO/LMO(2 nm)/STON junction, measured with and without magnetic field. Solid lines are guides for the eye.

6 nm. For the first junction, the MR is $\sim 91\%$ at $T=50$ K, and nearly linearly decreases to $\sim 30\%$ as temperature approaches 350 K. It is interesting that the MR effect remains significant even at the temperatures much greater than T_c [top inset in Fig. 2(a)]. The MR displays a monotonic increase with applied field at a fixed temperature, and there is no tendency to saturation up to 5 T [bottom inset in Fig. 2(a)]. Effects of electric biases on MR are quite weak, and only a slight decrease in MR as V grows occurs. The MR of the second junction is relatively low, and the maximal MR is only $\sim 27\%$. The most remarkable feature for this junction is the two-step MR–V behavior. The MR undergoes a sharp drop at a critical voltage, suggesting the different magnetic responses of the two processes. Figure 3(a) is a summary of the MR effect in different junctions. The MR is low when t is small, grows monotonically as layer thickness increases from 1 to 3 nm, decreases when t exceeds 4 nm, and vanishes above ~ 7 nm.

Positive MR also occurs under negative biases. It is small in both the high and low bias ranges, and gets a maximum of $\sim 150\%$ around -3 V. These behaviors are similar to those observed in $\text{CaMnO}_3/\text{STON}$,⁶ and could be ascribed to the depression of impact ionization by magnetic field.⁷ In the following we will focus on the MR under forward biases. In general, the MR of the manganite junctions is negative, and usually appears in heavily hole/electron-doped junctions, for which tunneling current determines the J–V characteristics. In this case, magnetic field can produce a reduction in depletion width of the junction, as demonstrated by the increase in capacitance.³ Different from the tunneling process, thermal process is insensitive to magnetic field, and the MR is quite low as observed in simple manganite junctions.^{3,4} The mechanism for the positive MR under positive biases, which is a combined effect of the LCMO/LMO and LMO/STON interfaces, may be completely different from those known at present. To get a deep understand of this phenomenon, it would be instructive to check the variation in the interfacial

potential (Φ_B) in magnetic field. To first approximation, LCMO/STON can be treated as a Schottky junction. In the presence of a LMO layer, according to Suzuki *et al.*,⁸ $(1-1/n)V$ is dropped across the insulating layer and V/n is applied to the depletion layer. This means the similarity of the J-V curves of LCMO/LMO/STON and LCMO/STON after describing the effect of the LMO layer by ideality factor, that is, $J \propto T^2 \exp(\Phi_B/k_B T) [\exp(eV/nk_B T) - 1]$.⁹ Based on this result, a direct calculation gives $J(0) - J(H) \propto \{\exp[-\Phi_B(0)/k_B T] - \exp[-\Phi_B(H)/k_B T]\} \exp(eV/nk_B T)$ and $MR \approx \exp\{[\Phi_B(H) - \Phi_B(0)]/k_B T\} - 1$. The former indicates a linear relation between $\log(\Delta J)$ and V , and the latter suggests a bias independence of the MR. These features can be clearly seen in the LCMO/LMO/STON junctions [Figs. 2 and 3(b)]. Based on these equations, the field-induced interfacial barrier change can be derived. Take the sample of $t=6$ nm at 230 K as an example. $\Delta\Phi_B$ is ~ 3.1 meV for the low bias process and ~ 2 meV for the high bias one, as magnetic field grows from 0 to 5 T. According to our previous letter,¹⁰ a notch and a spike occur in the conduction-band edges at the interface in the junction of $t=6$ nm, yielding two different processes in the high and the low bias ranges, respectively. It is interesting to note the different responses of the two processes to magnetic field. Similar analysis can be applied to other samples, and Fig. 3(c) shows the $\Delta\Phi_B - t$ curve thus obtained for $T=230$ K. With the decrease of temperature, Φ_B shows a gradual decrease. The resemblance between $\Delta\Phi_B - t$ and $MR - t$ reveals the close relation between the MR effect and interfacial potential growth, and it is the growth of the interfacial barrier that is responsible for the abnormal magnetic field effect in LCMO/LMO/STON.

Information about the interface can also be obtained from the capacitance (C)-voltage characteristics. Figure 3(d) exemplifies the bias dependence of the capacitance of LCMO/LMO(3 nm)/STON, measured under a frequency of 200 kHz. As expected, an approximately linear relation $1/C^2 - V$ is detected when $|V|$ is not large. This is a typical behavior of a Schottky junction, and the diffusion potential (V_d) can be obtained by extrapolating $1/C^2$ to zero. It shows that the field-induced change in diffusion potential varies between ~ 0.01 and 0.02 eV in the temperature range from 230 to 350 K ($\Phi_B \approx V_d + k_B T/e$). Although it is somewhat larger than that obtained from the J-V analyses, it confirms the increase in interfacial potential in magnetic field. It is obvious that an accurate analysis of the C-V characteristics should take into account the effect of the LMO layer. In this case, the voltage drop will be approximated by V/n , on the depletion layer, and $(1-1/n)V$, on the LMO layer. Correspondingly, the diffusion potential is determined by the $1/n^2 C^2 - V/n$ relation.⁸ Because of the small deviation of the ideality factor from unity at high temperatures, the $\Delta\Phi_B$ values thus obtained are essentially the same as those given above. As a supplement, we would like to point out that the

capacitance decreases in magnetic field. This phenomenon is different from that observed in $\text{La}_{0.7}\text{Sr}_{0.3}\text{MnO}_3/\text{STON}$ in which a negative MR occurred.³

We noted that an improved interface ferromagnetic ordering, due to the proximity effect has been observed in LSMO/LMO/STO. As shown by Yamada *et al.*,⁵ a LMO layer a few unit-cell in thickness has significantly enhanced the magnetic response of the interface layer. We also noticed a report on the variation in Fermi level accompanying a paramagnetic-ferromagnetic transition in LCMO,¹¹ presumably due to the band gap collapse as the FM order establishes. With these in mind, we propose that the MR observed here is due to the LMO/STON interface. Here the LMO layer behaves just like a deadlayer in the hole-doped manganite.¹² It could experience a change in magnetic order under magnetic field, which is possible considering the fact that the LMO layer may be effectively doped by LCMO due to proximity effect. This would in turn cause a reduction in Fermi level of the LMO layer, thus a growth in the interfacial barrier of LCMO/LMO/STON. Noting that the transport behavior of the junctions is mainly determined by the LMO/STON interface, it explains why the junction has MR effect but no clear ferromagnetic transition. As the thickness of the LMO layer increases, the effective doping is reduced since the proximity effect is limited to the LCMO/LMO interface, and therefore the MR effect disappears.

This work has been supported by the National Natural Science Foundation of China, the National Fundamental Research of China, and the Knowledge Innovation Project of the Chinese Academy of Sciences.

¹*Colossal Magnetoresistive Oxides*, edited by Y. Tokura (Gordon and Breach, London, 1999).

²J. Z. Sun, D. W. Abraham, R. A. Rao, and C. B. Eom, *Appl. Phys. Lett.* **74**, 3017 (1999); M. Bibes, S. Valencia, L. Balcells, B. Martínez, J. Fontcuberta, M. Wojcik, S. Nadolski, and E. Jedryka, *Phys. Rev. B* **66**, 134416 (2002).

³N. Nakagawa, M. Asai, Y. Mukunoki, T. Susaki, and H. Y. Hwang, *Appl. Phys. Lett.* **86**, 082504 (2005).

⁴D. J. Wang, J. R. Sun, Y. W. Xie, W. M. Lü, S. Liang, T. Y. Zhao, and B. G. Shen, *Appl. Phys. Lett.* **91**, 062503 (2007).

⁵H. Yamada, Y. Ogawa, Y. Ishii, H. Sato, M. Kawasaki, H. Akoh, and Y. Tokura, *Science* **305**, 646 (2004).

⁶C. M. Xiong, Y. G. Zhao, B. T. Xie, P. L. Lang, and K. J. Jin, *Appl. Phys. Lett.* **88**, 193507 (2006).

⁷J. J. H. M. Schoonus, F. L. Bloom, W. Wagemans, H. J. M. Swagten, and B. Koopmans, *Phys. Rev. Lett.* **100**, 127202 (2008).

⁸S. Suzuki, T. Yamamoto, H. Suzuki, K. Kawaguchi, K. Takahashi, and Y. Yoshisato, *J. Appl. Phys.* **81**, 6830 (1997).

⁹S. M. Sze and K. K. Ng, *Physics of Semiconductor Devices*, 3rd ed. (Wiley, New Jersey, 2007).

¹⁰W. M. Lü, J. R. Sun, Y. Z. Chen, and B. G. Shen, *Appl. Phys. Lett.* **94**, 152514 (2009).

¹¹J.-H. Park, C. T. Chen, S.-W. Cheong, W. Bao, G. Meigs, V. Chakarian, and Y. U. Idzerda, *Phys. Rev. Lett.* **76**, 4215 (1996).

¹²Y. H. Sun, Y. G. Zhao, H. F. Tian, C. M. Xiong, B. T. Xie, M. H. Zhu, S. Park, W. Wu, J. Q. Li, and Q. Li, *Phys. Rev. B* **78**, 024412 (2008).